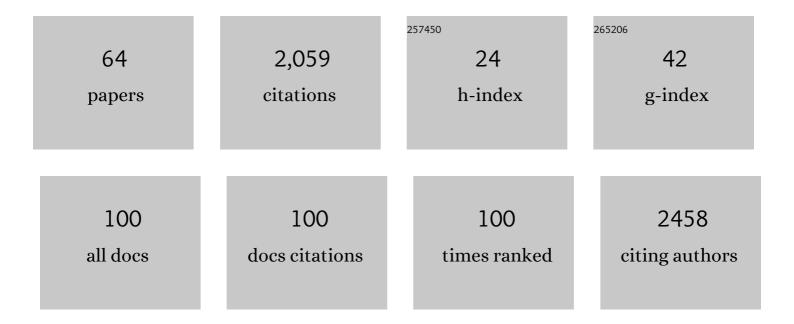
## Matthias Palm

List of Publications by Year in descending order

Source: https://exaly.com/author-pdf/1048928/publications.pdf Version: 2024-02-01



Μλττμίλς Ρλιμ

#	Article	IF	CITATIONS
1	Long-Term Observations of Atmospheric Constituents at the First Ground-Based High-Resolution Fourier-Transform Spectrometry Observation Station in China. Engineering, 2023, 22, 201-214.	6.7	5
2	Global Atmospheric OCS Trend Analysis From 22 NDACC Stations. Journal of Geophysical Research D: Atmospheres, 2022, 127, .	3.3	12
3	Spaceborne tropospheric nitrogen dioxide (NO <sub>2</sub> ) observations from 2005–2020 over the Yangtze River Delta (YRD), China: variabilities, implications, and drivers. Atmospheric Chemistry and Physics, 2022, 22, 4167-4185.	4.9	7
4	Satellite Observations Reveal a Large CO Emission Discrepancy From Industrial Point Sources Over China. Geophysical Research Letters, 2022, 49, .	4.0	7
5	A dataset of microphysical cloud parameters, retrieved from Fourier-transform infrared (FTIR) emission spectra measured in Arctic summer 2017. Earth System Science Data, 2022, 14, 2767-2784.	9.9	2
6	First retrievals of peroxyacetyl nitrate (PAN) from ground-based FTIR solar spectra recorded at remote sites, comparison with model and satellite data. Elementa, 2021, 9, .	3.2	7
7	Characterization and potential for reducing optical resonances in Fourier transform infrared spectrometers of the Network for the Detection of Atmospheric Composition Change (NDACC). Atmospheric Measurement Techniques, 2021, 14, 1239-1252.	3.1	9
8	COVIDâ€19 Crisis Reduces Free Tropospheric Ozone Across the Northern Hemisphere. Geophysical Research Letters, 2021, 48, e2020GL091987.	4.0	51
9	Mapping the drivers of formaldehyde (HCHO) variability from 2015 to 2019 over eastern China: insights from Fourier transform infrared observation and CEOS-Chem model simulation. Atmospheric Chemistry and Physics, 2021, 21, 6365-6387.	4.9	20
10	The Diurnal Variation in Stratospheric Ozone from MACC Reanalysis, ERA-Interim, WACCM, and Earth Observation Data: Characteristics and Intercomparison. Atmosphere, 2021, 12, 625.	2.3	5
11	The reduction in C <sub>2</sub> H <sub>6</sub> from 2015 to 2020 over Hefei, eastern China, points to air quality improvement in China. Atmospheric Chemistry and Physics, 2021, 21, 11759-11779.	4.9	12
12	Validation of methane and carbon monoxide from Sentinel-5 Precursor using TCCON and NDACC-IRWG stations. Atmospheric Measurement Techniques, 2021, 14, 6249-6304.	3.1	57
13	The drivers and health risks of unexpected surface ozone enhancements over the Sichuan Basin, China, in 2020. Atmospheric Chemistry and Physics, 2021, 21, 18589-18608.	4.9	12
14	Observed Hemispheric Asymmetry in Stratospheric Transport Trends From 1994 to 2018. Geophysical Research Letters, 2020, 47, e2020GL088567.	4.0	13
15	Fourier transform infrared time series of tropospheric HCN in eastern China: seasonality, interannual variability, and source attribution. Atmospheric Chemistry and Physics, 2020, 20, 5437-5456.	4.9	17
16	Detection and attribution of wildfire pollution in the Arctic and northern midlatitudes using a network of Fourier-transform infrared spectrometers and GEOS-Chem. Atmospheric Chemistry and Physics, 2020, 20, 12813-12851.	4.9	26
17	TROPOMI–Sentinel-5 Precursor formaldehyde validation using an extensive network of ground-based Fourier-transform infrared stations. Atmospheric Measurement Techniques, 2020, 13, 3751-3767.	3.1	66
18	Investigation of Arctic middle-atmospheric dynamics using 3 years of H <sub>2</sub> O and O <sub>3</sub> measurements from microwave radiometers at Ny-Ãlesund. Atmospheric Chemistry and Physics, 2019, 19, 9927-9947.	4.9	3

MATTHIAS PALM

#	Article	IF	CITATIONS
19	Ground-based millimetre-wave measurements of middle-atmospheric carbon monoxide above Ny-Ålesund (78.9° N, 11.9° E). Atmospheric Measurement Techniques, 2019, 12, 4077-4089.	3.1	1
20	An intercomparison of total column-averaged nitrous oxide between ground-based FTIR TCCON and NDACC measurements at seven sites and comparisons with the GEOS-Chem model. Atmospheric Measurement Techniques, 2019, 12, 1393-1408.	3.1	17
21	TCCON and NDACC X <sub>CO</sub> measurements: difference, discussion and application. Atmospheric Measurement Techniques, 2019, 12, 5979-5995.	3.1	19
22	The Arctic Cloud Puzzle: Using ACLOUD/PASCAL Multiplatform Observations to Unravel the Role of Clouds and Aerosol Particles in Arctic Amplification. Bulletin of the American Meteorological Society, 2019, 100, 841-871.	3.3	145
23	FTIR time series of stratospheric NO <sub>2</sub> over Hefei, China, and comparisons with OMI and GEOS-Chem model data. Optics Express, 2019, 27, A1225.	3.4	32
24	Assessing the ability to derive rates of polar middle-atmospheric descent using trace gas measurements from remote sensors. Atmospheric Chemistry and Physics, 2018, 18, 1457-1474.	4.9	18
25	Diurnal variation in middle-atmospheric ozone observed by ground-based microwave radiometry at Ny-Ãlesund over 1 year. Atmospheric Chemistry and Physics, 2018, 18, 4113-4130.	4.9	11
26	Ozone seasonal evolution and photochemical production regime in the polluted troposphere in eastern China derived from high-resolution Fourier transform spectrometry (FTS) observations. Atmospheric Chemistry and Physics, 2018, 18, 14569-14583.	4.9	42
27	Atmospheric CO and CH <sub>4</sub> time series and seasonal variations on Reunion Island from ground-based in situ and FTIR (NDACC and TCCON) measurements. Atmospheric Chemistry and Physics, 2018, 18, 13881-13901.	4.9	31
28	NDACC harmonized formaldehyde time series from 21 FTIR stations covering a wide range of column abundances. Atmospheric Measurement Techniques, 2018, 11, 5049-5073.	3.1	37
29	The influence of instrumental line shape degradation on NDACC gas retrievals: total column and profile. Atmospheric Measurement Techniques, 2018, 11, 2879-2896.	3.1	21
30	Continuous measurements of SiF 4 and SO 2 by thermal emission spectroscopy: Insight from a 6-month survey at the Popocatépetl volcano. Journal of Volcanology and Geothermal Research, 2017, 341, 255-268.	2.1	20
31	Measuring atmospheric ammonia with remote sensing campaign: Part 1 – Characterisation of vertical ammonia concentration profile in the centre of The Netherlands. Atmospheric Environment, 2017, 169, 97-112.	4.1	29
32	Technical note: Sensitivity of instrumental line shape monitoring for the ground-based high-resolution FTIR spectrometer with respect to different optical attenuators. Atmospheric Measurement Techniques, 2017, 10, 989-997.	3.1	13
33	The arctic seasonal cycle of total column CO <sub>2</sub> and CH <sub>4</sub> from ground-based solar and lunar FTIR absorption spectrometry. Atmospheric Measurement Techniques, 2017, 10, 2397-2411.	3.1	4
34	Validation of the CrIS fast physical NH <sub>3</sub> retrieval with ground-based FTIR. Atmospheric Measurement Techniques, 2017, 10, 2645-2667.	3.1	52
35	Atmospheric inverse modeling via sparse reconstruction. Geoscientific Model Development, 2017, 10, 3695-3713.	3.6	6
36	Tropospheric water vapour isotopologue data (H <sub>2</sub> <sup>16</sup> O,) Tj ETQq0 0 0 1	gBT /Overl 9.9	ock 10 Tf 50 ( 26

Earth System Science Data, 2017, 9, 15-29.

MATTHIAS PALM

#	Article	IF	CITATIONS
37	Strato-mesospheric carbon monoxide profiles above Kiruna, Sweden (67.8 º N, 20.4 º E), since 2008. System Science Data, 2017, 9, 77-89.	Earth <sub>9.9</sub>	5
38	Retrieval of xCO <sub>2</sub> from ground-based mid-infrared (NDACC) solar absorption spectra and comparison to TCCON. Atmospheric Measurement Techniques, 2016, 9, 577-585.	3.1	18
39	Stratospheric aerosol-Observations, processes, and impact on climate. Reviews of Geophysics, 2016, 54, 278-335.	23.0	265
40	Towards understanding the variability in biospheric CO <sub>2</sub> Âfluxes: using FTIR spectrometry and a chemical transport model to investigate the sources and sinks of carbonyl sulfide and its link to CO <sub>2</sub> . Atmospheric Chemistry and Physics, 2016, 16, 2123-2138.	4.9	20
41	An evaluation of IASI-NH <sub>3</sub> with ground-based Fourier	4.9	56
42	Positive trends in Southern Hemisphere carbonyl sulfide. Geophysical Research Letters, 2015, 42, 9473-9480.	4.0	20
43	Trends of ozone total columns and vertical distribution from FTIR observations at eight NDACC stations around the globe. Atmospheric Chemistry and Physics, 2015, 15, 2915-2933.	4.9	76
44	Retrieval of ammonia from ground-based FTIR solar spectra. Atmospheric Chemistry and Physics, 2015, 15, 12789-12803.	4.9	32
45	Using XCO <sub>2</sub> retrievals for assessing the long-term consistency of NDACC/FTIR data sets. Atmospheric Measurement Techniques, 2015, 8, 1555-1573.	3.1	39
46	Multistation intercomparison of column-averaged methane from NDACC and TCCON: impact of dynamical variability. Atmospheric Measurement Techniques, 2014, 7, 4081-4101.	3.1	22
47	Tropospheric CH <sub>4</sub> signals as observed by NDACC FTIR at globally distributed sites and comparison to GAW surface in situ measurements. Atmospheric Measurement Techniques, 2014, 7, 2337-2360.	3.1	38
48	Recent Northern Hemisphere stratospheric HCl increase due to atmospheric circulation changes. Nature, 2014, 515, 104-107.	27.8	110
49	On the impact of the temporal variability of the collisional quenching process on the mesospheric OH emission layer: a study based on SD-WACCM4 and SABER. Atmospheric Chemistry and Physics, 2014, 14, 10193-10210.	4.9	12
50	Year-round retrievals of trace gases in the Arctic using the Extended-range Atmospheric Emitted Radiance Interferometer. Atmospheric Measurement Techniques, 2013, 6, 1549-1565.	3.1	6
51	Influence of Solar Radiation on the Diurnal and Seasonal Variability of O3 and H2O in the Stratosphere and Lower Mesosphere, Based on Continuous Observations in the Tropics and the High Arctic. Springer Atmospheric Sciences, 2013, , 125-147.	0.3	5
52	Ground-based remote sensing of tropospheric water vapour isotopologues within the project MUSICA. Atmospheric Measurement Techniques, 2012, 5, 3007-3027.	3.1	69
53	CO at 40–80 km above Kiruna observed by the ground-based microwave radiometer KIMRA and simulated by the Whole Atmosphere Community Climate Model. Atmospheric Chemistry and Physics, 2012, 12, 3261-3271.	4.9	18
54	Observed and simulated time evolution of HCl, ClONO <sub>2</sub> , and HF total column abundances. Atmospheric Chemistry and Physics, 2012, 12, 3527-3556.	4.9	72

MATTHIAS PALM

#	Article	IF	CITATIONS
55	Calibration of column-averaged CH <sub>4</sub> over European TCCON FTS sites with airborne in-situ measurements. Atmospheric Chemistry and Physics, 2012, 12, 8763-8775.	4.9	55
56	Calibration of TCCON column-averaged CO <sub>2</sub> : the first aircraft campaign over European TCCON sites. Atmospheric Chemistry and Physics, 2011, 11, 10765-10777.	4.9	120
57	Observation of strato-mesospheric CO above Kiruna with ground-based microwave radiometry – retrieval and satellite comparison. Atmospheric Measurement Techniques, 2011, 4, 2389-2408.	3.1	30
58	Validation of five years (2003–2007) of SCIAMACHY CO total column measurements using ground-based spectrometer observations. Atmospheric Measurement Techniques, 2010, 3, 1457-1471.	3.1	31
59	The ground-based MW radiometer OZORAM on Spitsbergen – description and status of stratospheric and mesospheric O <sub>3</sub> -measurements. Atmospheric Measurement Techniques, 2010, 3, 1533-1545.	3.1	37
60	Ozone profile retrieval from limb scatter measurements in the HARTLEY bands: further retrieval details and profile comparisons. Atmospheric Chemistry and Physics, 2008, 8, 2509-2517.	4.9	6
61	Intercomparison of O <sub>3</sub> profiles observed by SCIAMACHY and ground based microwave instruments. Atmospheric Chemistry and Physics, 2005, 5, 2091-2098.	4.9	15
62	Starting long-term stratospheric observations with RAMAS at Summit, Greenland. IEEE Transactions on Geoscience and Remote Sensing, 2005, 43, 1022-1027.	6.3	4
63	Efficient solution of boundary-value problems for image reconstruction via sampling. Journal of Electronic Imaging, 2000, 9, 251.	0.9	4
64	<title>Efficient exact PDE solutions for MCMC</title> ., 1999, , .		1

<title>Efficient exact PDE solutions for MCMC</title>. , 1999, , . 64